**Article ID:** 1003－6326(2004)02－0270－04

# Subsolidus binary phase diagram of $C_{10}Zn$-$C_{18}Zn$ of thermotropic phase transitions materials①

WU Ke-zhong(武克忠)[1,2], WANG Xin-dong(王新东)[2], LIU Xiao-di(刘晓地)[1], ZUO Ping(左 萍)[1]
(1. Department of Chemistry, Hebei Normal University, Shijiazhuang 050016, China;
2. Department of Physical Chemistry, University of Science and Technology Beijing, Beijing 100083, China)

**Abstract:** The thermotropic phase transitions layer compound in the perovskite type $(n\text{-}C_{10}H_{21}NH_3)_2ZnCl_4$ and $(n\text{-}C_{18}H_{37}NH_3)_2ZnCl_4$ were synthesized and, at the same time, a series of mixtures $C_{10}Zn/C_{18}Zn$ were prepared. The experimental binary phase diagram of $C_{10}Zn/C_{18}Zn$ was established by means of differential scanning calorimetry (DSC) and X-ray diffraction. In the phase diagram, compound $(n\text{-}C_{10}H_{21}NH_3)(n\text{-}C_{21}H_{37}NH_3)ZnCl_4$ and two eutectoid invariants were observed; two eutectoid temperatures are about 53 ℃ and 58 ℃. Contrasting with other similar systems, there are three noticeable solid solution ranges at the left and right boundary and middle of the phase diagram.

**Key words:** decylammonium tetrachlorozincate; octadecylammonium tetrachlorozincate; phase diagram
**CLC number:** TQ 266; O 642.31 **Document code:** A

## 1 INTRODUCTION

$A_2BX_4$ or $ABX_3$ type compounds (A represents metal, and X halogen or oxygen) have attracted considerable attention because of their physical properties, including ferro-, piezo- or pyroelectricity, ferri-, antiferro- or piezomagnetism and non-linear optical effects, and their technical applications to electro- or magneto-optical devices[1, 2]. Similar physical properties and structures are observed when metal A is substituted by an $[NR_4]^+$ ion (R represents H, alkyl, or aryl)[3-6]. In order to search for new materials with electro-optic effects, we have synthesized two materials which belong to $[NR_4]_2ZnCl_4$ in bis($n$-alkylammonium) tetrachlorozincates (Ⅱ) with the general formula $(n\text{-}C_{10}H_{21}\text{-}NH_3)_2ZnCl_4$ (short notation: $C_{10}M$) and $(n\text{-}C_{18}\text{-}H_{37}NH_3)_2ZnCl_4$ (short notation: $C_{18}M$). Two compounds are known to crystallize in a bidimensional structure of perovskite. The bidimensional macroanions of $MCl_4^{2-}$ are sandwiched between double layers of $n$-alkylammonium cations. The layers were bound by van der Waals forces between $CH_3$ groups and by long-range Coulomb forces. The cavities in the tetrahedral were occupied by the $-NH_3^+$ polar head of the $n$-alkylammonium cations which form weak N—H …Cl hydrogen bonds with the halogens. The physical properties and structure of $C_nM$ have been previously investigated[6-13]. Busico et al[14] studied binary $C_nZn$ systems. The binary phase diagram for $C_nM$ is reported elsewhere[15], except for $C_{10}Zn/C_{18}Zn$. In this paper the subsolidus binary phase diagram of $C_{10}Zn/C_{18}Zn$ is obtained by using DSC and X-ray diffraction. The phase diagram of $C_{10}Zn/C_{18}Zn$ is different from that of similar system in the literature.

## 2 EXPERIMENTAL

$ZnCl_2$, concentrated HCl and absolute ethanol used were analytical grade. Decylamine was purchased from Beijing Xudong Chemical Plant, China, octadecylamine from Development Center of Special Reagent of North China.

$C_{10}Zn$ and $C_{18}Zn$ were prepared according to previous report[14] and analyzed with an MT-3 CHN elemental analyzer (Japan). The results of elemental analysis in mass fraction (%) are, $C_{10}Zn$: C 45.68 (45.861), H 9.27(9.24), N 5.27(5.35); $C_{18}Zn$: C 58.26 (57.79), H 10.26(10.78), N 4.26(3.74) (note: experimental value (calculated value)). The products, $C_{10}Zn$ and $C_{18}Zn$, were weighed exactly in desired proportions to prepare different mixed samples. The two components were dissolved in absolute ethanol, and then part of the solvent was evaporated. Air-dried samples were put into a vacuum desiccator at about 80 ℃ for 8 h.

The thermal behavior of the samples was determined with a CDR-1 differential scanning calorimeter

① **Foundation item:** Project(202139) supported by the Natural Science Foundation of Hebei Province, China; project(50074003) supported by the National Natural Science Foundation of China
**Received date:** 2003－06－16; **Accepted date:** 2003－10－16
**Correspondence:** LIU Xiao-di, Professor; Tel: +86-311-6268160; E-mail: liuxiaodi1@263.net

(DSC; Shanghai Scale Instrument Plant, China) at a scanning rate of 5 ℃/min in a steady atmosphere. Samples weighing about 5 mg were sealed in aluminum crucibles.

X-ray diffraction patterns on compacted power samples of the powders were taken by D/MAX-RA X-ray diffractometer(made in Japan), under the conditions of Cu $K_\alpha$, Ni filter, scanning rate of 2(°)/min, voltage 40 kV and electric current 100 mA.

## 3 EXPERIMENTAL RESULTS

### 3.1 Thermal analysis

The experimental results of DSC after treatment with "Shape factors method"[16] were listed in Table 1. Fig. 1 shows the DSC curves of the $C_{10}$-Zn, $C_{18}Zn$ and their mixtures. Data show that with increasing $w$($C_{10}Zn$), the transition temperature of the system decreases. The first eutectoid temperature at about 53 ℃ appears in the range of 14.75%–28.40% $C_{10}Zn$. The transition temperature firstly rises, then drops. The second eutectoid temperature at about 58 ℃ is found from 46.81% to 86.71% $C_{10}Zn$. With $w$($C_{10}Zn$) increasing gradually, the phase transformation temperature rises again. Table 1 reveals that the first eutectoid temperature is not observed close to $w$($C_{12}Zn$) = 0, nor does the second end near $w$($C_{10}Zn$) = 100%. The range of the first eutectoid temperature does not end close to the beginning of the second one. These observations indicate miscibility region at the left and right boundary and middle of the phase diagram.

**Table 1** Solid-solid transition temperature of $C_{10}Zn$-$C_{18}Zn$ system

| $w$($C_{10}Zn$)/% | $t_{e1}$/℃ | $t_{e2}$/℃ | $t_o$/℃ | $t_f$/℃ |
|---|---|---|---|---|
| 0($C_{18}Zn$) | | | 89 | |
| 8.66 | | | 68 | 85 |
| 14.75 | 52 | | | 79 |
| 19.12 | 53 | | | 70 |
| 28.40 | 53 | | | 77 |
| 37.83 | | | 68 | 79 |
| 40.07 | | | 77 | 80 |
| 46.81 | | 59 | | 77 |
| 55.79 | | 58 | | 77 |
| 61.55 | | 58 | | 78 |
| 67.90 | | 59 | | 68 |
| 79.20 | | 58 | | 77 |
| 86.71 | | 57 | | 78 |
| 92.75 | | | 67 | 79 |
| 100($C_{10}Zn$) | | | 81 | |

$t_e$—eutectoid invariant; $t_o$—onset temperature; $t_f$—finish temperature

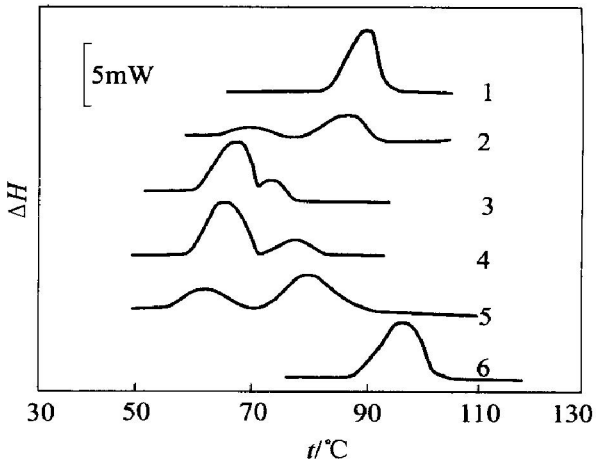


**Fig. 1** DSC curves of binary systems of $C_{10}Zn$-$C_{18}Zn$
1—$C_{10}Zn$; 2—55.17% $C_{10}Zn$; 3—67.90% $C_{10}Zn$; 4—74.10% $C_{10}Zn$; 5—83.63% $C_{10}Zn$; 6—$C_{18}Zn$

### 3.2 X-ray diffraction

X-ray diffraction patterns are convenient for phase analysis, because the interplanar spacing $d$ and relative intensity $I$ are intrinsic properties of substances. Fig. 2 and Fig. 3 show the X-ray diffraction patterns of $C_{10}Zn$ and $C_{18}Zn$. Table 2

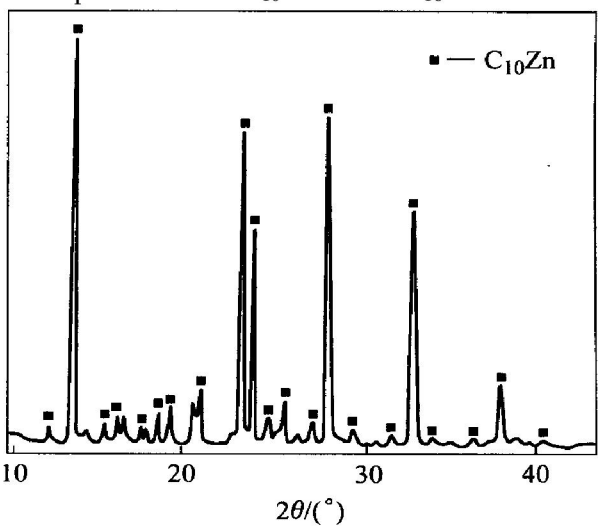


**Fig. 2** XRD pattern of $C_{10}Zn$

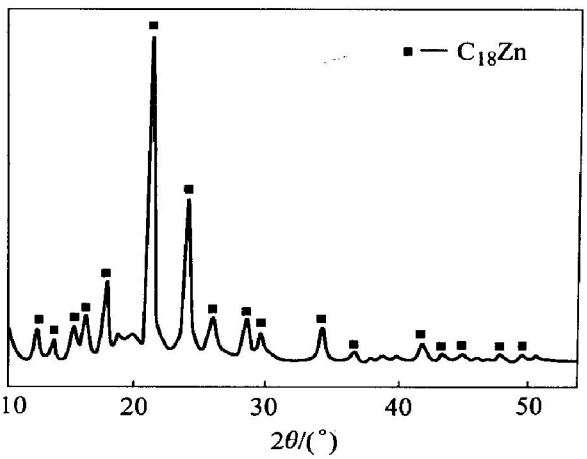


**Fig. 3** XRD pattern of $C_{18}Zn$

**Table 2** $d$ values at room temperature

| $C_{18}Zn$ | $w(C_{10}Zn)$ | | | | | | | | | $C_{10}Zn$ |
|---|---|---|---|---|---|---|---|---|---|---|
| | 8.66% | 14.75% | 28.40% | 40.07% | 46.81% | 61.55% | 79.20% | 86.71% | 92.75% | |
| 7.054 | 7.054 | 7.056 | 7.045 | 6.267 | 6.879 | 6.888 | 6.911 | 6.931 | 6.949 | 6.915 |
| 6.528 | 6.638 | 6.612 | 6.640 | 5.569 | 6.251 | 6.249 | 6.216 | 6.231 | 6.258 | 6.227 |
| 5.901 | 6.016 | 6.016 | 6.016 | 4.516 | 5.571 | 5.570 | 5.547 | 5.562 | 5.996 | 5.971 |
| 5.456 | 5.838 | 5.838 | 5.823 | 4.175 | 5.369 | 5.331 | 5.327 | 5.327 | 5.572 | 5.549 |
| 4.961 | 5.544 | 5.544 | 5.537 | 3.674 | 4.484 | 4.884 | 4.971 | 4.976 | 5.361 | 5.349 |
| 4.128 | 5.056 | 5.037 | 5.029 | 3.412 | 4.506 | 4.510 | 4.845 | 4.850 | 4.876 | 5.206 |
| 3.644 | 4.790 | 4.804 | 4.518 | 3.116 | 3.764 | 3.757 | 4.497 | 4.521 | 4.688 | 4.967 |
| 3.422 | 4.178 | 4.518 | 4.178 | 2.680 | 3.648 | 3.670 | 4.234 | 4.213 | 4.518 | 4.678 |
| 3.061 | 3.679 | 4.183 | 3.679 | 2.629 | 3.541 | 3.524 | 4.149 | 4.151 | 4.268 | 4.502 |
| 2.937 | 3.420 | 3.680 | 3.100 | 2.444 | 3.490 | 3.412 | 3.740 | 3.740 | 4.164 | 4.262 |
| 2.537 | 3.090 | 3.420 | 2.628 | 2.020 | 3.410 | 3.102 | 3.657 | 3.652 | 3.753 | 4.150 |
| 2.087 | 2.559 | 3.095 | 2.558 | | 3.112 | 2.664 | 3.518 | 3.512 | 3.673 | 3.741 |
| | | 2.628 | 2.393 | | 2.665 | 2.515 | 3.408 | 3.401 | 3.529 | 3.660 |
| | | 2.391 | 2.203 | | 2.510 | 2.208 | 3.206 | 3.214 | 3.418 | 3.522 |
| | | | | | 2.200 | 2.068 | 3.112 | 3.112 | 3.217 | 3.403 |
| | | | | | 1.817 | 1.866 | 2.978 | 2.879 | 3.122 | 3.210 |
| | | | | | | | 2.769 | 2.562 | 2.988 | 3.116 |
| | | | | | | | 2.583 | 2.416 | 2.783 | 2.983 |

summarizes the $d$ values of strong peaks with bigger relative intensity at room temperature for pure $C_{10}Zn$, $C_{18}$-Zn and their mixtures. We find $d$ values of samples with composition from 8.66% to 14.75 % $C_{10}$ Zn are similar to those of pure $C_{18}$Zn. This shows that they are in a single-phase region. That is to say, in this content range, $C_{10}C_{18}Zn$ dissolves in $C_{18}Zn$ to form a solid solution(α). Similarly, samples with composition from 92.75% to 100% $C_{10}Zn$ have homologous patterns showing that $C_{10}C_{18}Zn$ dissolves in $C_{10}Zn$ to form a solid solution(β). In the same way, samples with composition from > 28.40% to 40.07% $C_{10}Zn$ are in a single-phase(γ), which is $C_{10}Zn$ or $C_{18}Zn$ dissolved in $C_{10}C_{18}Zn$. Samples with composition from 14.75% to 28.40% $C_{10}Zn$ are in the two-phase region, and their patterns are the overlap of α and γ. The patterns of 46.81% to 86.71% $C_{10}Zn$ are the overlap of β and γ in the two-phase region. These facts indicate that the $C_{10}Zn$-$C_{18}Zn$ phase diagram has partial miscibility regions.

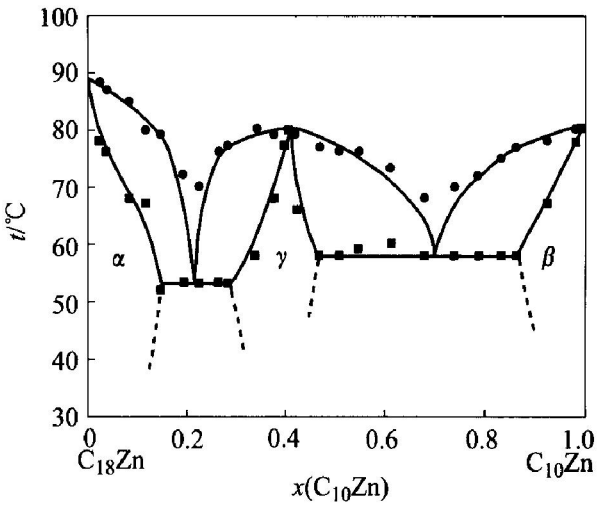


**Fig. 4** Binary phase diagram of $C_{10}Zn$/$C_{18}Zn$

## 4 DISCUSSION

Fig. 4 indicates an intermediate $(C_{10}H_{21}NH_3)$-$(C_{18}H_{37}NH_3)ZnCl_4$ is formed, because there is a top temperature between two eutectoid invariants[17]. At room temperature, the pure salts and their mixtures are ordered. Alkylammonium chains are parallel to each other and slightly tilted with respect to the normal to the inorganic layers, and the chains are hydrogen bonded to $ZnCl_4^{2-}$. When the temperature goes up, the first eutectoid invariant occurs at 53 ℃ from 14.757% to 28.40% $C_{10}Zn$. $C_{10}Zn$ and $C_{12}C_{18}Zn$

undergo a reversible solid-solid phase transformation. In this situation, the chains are in a large degree of motional freedom and a disordered phase appears. At the same time, the hydrogen bonds are weakened and even destroyed. When the temperature continues to increase, the second eutectoid invariant at 58 ℃ appears from 46.81% to 86.71% $C_{10}Zn$. Similarly $C_{18}Zn$ and $C_{10}C_{18}Zn$ undergo a reversible solid-solid phase transformation.

A binary phase diagram for a homologous system was reported[15], and the shape is similar to ours. The largest difference is that their diagram shows absolute immiscibility, but ours, partial miscibility. Binary system phase diagrams are determined by the difference of two components. If their structure and size have little difference, they often dissolve each other and form miscible system. Conversely, when they have much difference, the degree of miscibility is limited. $C_{10}C_{18}Zn$ can be looked as $C_{10}Zn$ and $C_{18}Zn$ with one chain exchanged, so their structure and molecular size have little difference, which results in their partial miscibility.

## REFERENCES


[1] West A R. Solid State Chemistry and its Application [M]. New York: John Wiley & Sons, 1984. 4-5.

[2] XIANG Y, XIE D H. Structure and characteristic of $ABO_3$-type oxide and its application[J]. Journal of Materials Engineering, 2000(9): 15-18. (in Chinese)

[3] Ciajolo M R, Corradini P, Pavone V. Comparative studied of layer structures: the crystal structure of bis (*n*-monodecylammonium) tetrachloromanganate (Ⅱ) [J]. Gazz Chim Ital, 1976, 106: 807-815.

[4] Schenk K J, Chapuis G. Thermotropic phase transitions in bis(*n*-tetradecylammonium) tetrachlorocadmate(Ⅱ) and some homologous compounds[J]. J Phys Chem, 1988, 92(25): 7141-7147.

[5] Jakubas R, Bator M, Gosniowska M, et al. Crystal structure and phase transition of $[(CH_3)_2NH_2]$ $GaCl_4$ [J]. J Phys Chem Solids, 1997, 58(6): 989-998.

[6] Avitabile G, Ciajolo M R, Napolitano R, et al. Comparative studies of layer structure: the crystal structures of bis(mono-*n*-docylammonium) tetrabromozincate and bis (mono-*n*-tridecylammonium) tetrabromozincate [J]. Gazz Chim Ital, 1983, 113: 475-479.

[7] Venkataraman N V, Barman S, Vasudevan S, et al. Structural analysis of alkyl chain conformation in the layered organic-inorganic hybrid $[(C_nH_{2n+1})\text{-}NH_3]_2PbI_4$ ($n$= 12, 16, 18) by spectroscopy[J]. Chem Phy Lett, 2002, 358: 139-143.

[8] Ciajolo M R, Corradini P, Pavone V. Bis(*n*-dodecylammomium) tetrachlorozincate[J]. Acta Cryst, 1977, B33: 553-555.

[9] Tabuchi Y, Asai K, Rikukawa M, et al. Preparation and characterization of natural low dimensional layered perovskite-type compounds[J]. J Phys Chem Solids, 2000, 61: 837-845.

[10] RUAN D S, ZHANG T P, ZHANG D S, et al. DSC investigation of phase change material[J]. New Energy Sources, 1994(4), 16: 19-24. (in Chinese)

[11] Fenrych J, Reynhardt E C, Jurga S, et al. Molecular motions and phase changes in the perovskite-type compound $(C_{10}H_{21}NH_3)_2ZnCl_4$ [J]. Molecular Physics, 1993, 78(5): 1117-1128.

[14] Busico V, Tartaglione T, Vacatello M. The thermal behavior of mixed long chain alkylammonium tetracholomanganates(Ⅱ)[J]. Thermochim Acta, 1983, 62: 77-86.

[15] LI W P, ZHANG D S, ZHANG T P, et al. Study of solid-solid phase change of $(n\text{-}C_nH_{2n}+1NH_3)_2MCl_4$ for thermal energy storge[J]. Thermochim Acta, 1999, 326: 183-186.

[16] Courchinoux R, Chanh N B, Haget Y. Use of the "shape factors" as an empirical method to determine the actual characteristic temperatures of binary phase diagrams by differential scanning calorimetry[J]. Thermochim Acta, 1988, 128: 45-53.

[17] Atkins P W. Physical Chemistry[M]. Oxford: Oxford University, 1990.


**(Edited by PENG Chao-qun)**